



Article citation info:

Pielecha I, Szwajca F. Cooperation of a PEM fuel cell and a NiMH battery at various states of its charge in a FCHEV drive. *Eksploracja i Niezawodność – Maintenance and Reliability* 2021; 23 (3): 468–475, <http://doi.org/10.17531/ein.2021.3.7>.

Cooperation of a PEM fuel cell and a NiMH battery at various states of its charge in a FCHEV drive

Ireneusz Pielecha^a, Filip Szwajca^a

^aPoznan University of Technology, Faculty of Civil and Transport Engineering, ul. Piotrowo 3, 60-965 Poznan, Poland

Indexed by:



Highlights

- Experimental analysis of energy flow in a hydrogen-electric propulsion system
- Increasing driving dynamics significantly reduces the share of energy from the fuel cell
- Full power operation of the system leads to energy transfer efficiency up to 95%
- Variable driving conditions result in operation with an efficiency of 64–75%

Abstract

The development of electromobility is focused on the design and implementation of increasingly more effective electric drives. In such a system, apart from energy recovery, it is not possible to recharge the batteries while driving. Electric vehicles equipped with fuel cells and a battery (FCHEV – fuel cell hybrid electric vehicle) in a parallel configuration boast increased energy transfer capabilities. The article presents an energy flow analysis in a parallel hybrid drive system with fuel cells and a battery. The research was carried out on a 30 W vehicle made in 1:10 scale with a NiMH battery and a fuel cell with a proton exchange membrane (PEM). Increasing driving dynamics causes a 29% increase in energy consumption, 43.6% reduction of energy transfer from a fuel cell and a 23% increase of in the energy share intended for battery charging. Continuous operation of the system in full power mode ensures a much greater efficiency of energy transmission to the drive train (95%) compared to the system operating in dynamic driving conditions – 64–75%.

Keywords

This is an open access article under the CC BY license (<https://creativecommons.org/licenses/by/4.0/>)

hybrid drive, fuel cells, energy flow, vehicle drive energy management.

1. Introduction

The search for substitutes for conventional fuels and vehicle drives contributes to the development of hybrid drives and electric drives. The testing procedures for typical internal combustion propulsion systems are increasingly more complicated (thanks to the introduction of stringent exhaust emission norms) and require both bench and road tests in real traffic conditions [7, 27]. The use of alternative drives (electric and hydrogen fuel) thus leads to a reduction in the environmental impact [24] and reduction of the carbon footprint of modern drive systems.

Hydrogen (H₂) can be used as a fuel for propulsion systems in two basic ways. The first one consists of hydrogen combustion in internal combustion engine (ICE) and direct conversion of chemical energy into mechanical energy [8, 25]. The second one is the production of electricity using hydrogen fuel cells, which is then used to drive the vehicle's electric motors [23]. In a parallel configuration with the battery, this solution provides wide possibilities of energy transfer between the individual drive system components.

Hydrogen-powered internal combustion engines can be used as single-fuel engines, or hydrogen can provide an additional dose of fuel when burned along with conventional fuel by using a direct or indirect injection system [17]. Hydrogen has several advantages when

it comes to its use in spark ignition engines. These include broad flammability limits, high auto-ignition temperature and minimal requirements of the energy initiating the combustion process when compared to gasoline or methane, which is the main component of natural gas [13]. Thanks to this, it is possible to increase the engine thermal efficiency by using lean mixtures combustion for example. Powering compression-ignition engines with pure hydrogen is problematic due to the high resistance to auto-ignition, however, using an additional source of energy or a very high compression ratio, this solution can be made applicable. A less problematic method of hydrogen combustion is the use of a dual-fuel combustion system, where a small pilot dose of diesel fuel plays the role of the combustion process initiator. The research results on hydrogen combustion in compression-ignition engines indicate a reduction in the exhaust emission of particulate matter, hydrocarbons, as well as carbon monoxide and dioxide. On the other hand, it led to an increase in the share of nitrogen oxides [11].

The advantage of using conventional combustion engines compared to fuel cell systems is the low cost of engine adaptation to hydrogen fuel [16] when compared to the price of fuel cells. Whereas other beneficial aspects of hydrogen energy sources clearly indicate the greater benefits of fuel cells, which are more efficient, do not emit toxic exhaust components, and their operation causes much lower noise emissions [29].

E-mail addresses: I. Pielecha - Ireneusz.Pielecha@put.poznan.pl, F. Szwajca - Filip.Szwajca@put.poznan.pl

In [4] a comparison of fuel consumption and exhaust emissions of three types of vehicles equipped with two different sources of conventional propulsion was made, an internal combustion engine cooperating with a fuel cell (ICE + PEMFC) and a fuel cell drive system (PEMFC – *proton exchange membrane fuel cell*) in WLTP (*Worldwide Harmonized Light-Duty Vehicles Test Procedure*) and NEDC (*New European Driving Cycle*) tests. The lowest fuel consumption in terms of gasoline consumption was achieved using the PEMFC fuel cell and reached the value of 3.61 dm³/100 km in the NEDC test (fuel consumption by ICE and ICE + PEMFC vehicles was higher by 24.6% and 20.5%, respectively). Hybridizing the drive system power source significantly reduced the exhaust emissions of carbon monoxide (CO), hydrocarbons (THC) and nitrogen oxides (NO_x) compared to the conventional drive system (ICE).

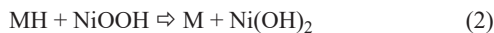
Vehicles equipped with a fuel cell as an energy source are built from the main power source and the energy storage system (ESS). The maximum system power (in relation to the parallel drive) is then given by the formula [14]:

$$P_{load}(t) = P_{FC\ sys}(t) + P_{ES\ sys}(t) \quad (1)$$

Nickel-metal hydride (*nickel-metal hydride*) batteries are widely used in hybrid and electric drives, which are commonly being replaced by lithium-ion (*Li-Ion*) batteries. The usefulness of hybrid drives in urban traffic conditions is confirmed both by their lower fuel consumption and by the effect they have on limiting the toxic exhaust emission components [4, 9, 28]. Nevertheless, NiMH batteries show better scalability in series connection, they do not require balancing of cells when connecting them, and have a greater voltage tolerance when charging. Li-Ion batteries are characterized by a higher voltage value of a single cell (2.3–4.8 V depending on the cathode and anode material [6]) compared to the voltage of 1.2 V in NiMH batteries. In addition, their electrical capacity is greater with the same size dimensions.

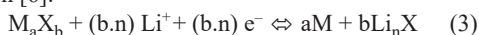
The general reactions during charging/discharging of batteries take the form

- for NiMH [20]:



where M is a hydrogen absorbing alloy;

- for Li-Ion [6]:



where M is a transition metal or a mixture of such metals, X is an anion from the oxygen, halogen, nitrogen, phosphorus, sulfur group etc. or a combination of several such anions, and n is the oxidation state of X.

NiMH batteries used in hybrid vehicles contain: about 36% steel, 23% nickel, 18% plastic, 9% electrolyte, 7% rare earth elements (4% cobalt and 3% of other materials) [20].

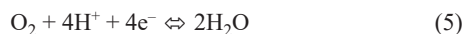
Currently, from among various types of fuel cells, the PEM type fuel cells are the solution dedicated to automotive use, due to their low operating temperature (about 80°C) and relatively high efficiency. The theoretical value of their efficiency reaches 75.7% for air-hydrogen cells [18, 22].

The electrochemical reactions and processes on the electrodes can be denoted as [31]:

- anode:



- cathode:



- total:



The analysis by Akinyele et al. [2] indicates a high specific power value in excess of 1000 W/kg, a specific energy value of 100–450 Wh/kg and a power density of over 3.8 kW/m³ for PEM cells.

There are three configurations of energy storage systems in FCHEV vehicles [27]:

- Fuel cell and ultracapacitor,
- Fuel cell and an electrochemical battery,
- Fuel cell, ultracapacitor and an electrochemical battery.

The use of ultracapacitors increases costs and lowers fuel economy, as opposed to systems using batteries, e.g. Li-Ion. Connecting ultracapacitors in parallel with batteries with appropriate optimization allows – apart from fuel economy – to extend the lifespan of the batteries [5].

Drive system design and control optimization efforts are currently pursued intensively. The simulations of hydrogen drive system optimization shows that it is possible to reduce the maximum cell current from 500 A to 100 A by using an ultracapacitor (in critical driving cycle situations, such as during acceleration). It also allows to reduce the battery pack's output power by approx. 20%. As a result, the simulation predicts a 3.3% reduction in fuel consumption [9].

Khayyer and Famouri [21] proposed to use two smaller fuel cells instead of a single large one. The simulations were based on fuel cells with a power of 35 and 50 kW, respectively, and batteries with a rated power of 36 kW. This resulted in significant energy savings for driving in urban conditions. On the other hand, the use of an island genetic model algorithm for the optimization of the energy management system (EMS), based on a fuzzy control system, allowed to achieve hydrogen consumption reduction by 1.1%–8.4% in four drive tests, which translated into an increase in range by 1.10–9.15 km per 100 km [32]. Similar effects were achieved by the use of EMS based on the prediction of traffic conditions and the use of the Hull Moving Average (HMA) algorithm and fuzzy logic, reducing hydrogen consumption by 0.1167 dm³/s [30].

Typical hybrid solutions using fuel cells and batteries require the voltage of both systems to be adjusted. The value of the fuel cell voltage needs to be adjusted to the decreasing battery voltage during its discharge [1, 12]. Hence, various types of DC-DC regulators are used [3]. Their efficiency is usually highest at maximum load. Their maximum performance capabilities are rarely achieved, especially when travelling in urban traffic conditions. There are many hybrid solutions that do not use such DC-DC converters. Such tests at a system voltage of 48 V were conducted by Shang et al. [26]. The work involved the use of a 3 kW fuel cell (43.2 V @ 70 A) and several battery variants: 4 × 12 V (lead-acid batteries), 16 × 3.4 V (Li-Ion batteries), 15 × 3.4 V (Li-Ion batteries). It has been found that the elimination of the DC-DC converter not only lowers the overall cost of the system, but also increases its efficiency. Unfortunately, the disadvantage of such a solution is the need to adjust the voltages of the cell stack, batteries and electric motors. It is also necessary to provide an appropriate battery charge/discharge curve to the fuel cell discharge curve. Only then will such a system ensure high operational efficiency.

Howroyd and Chen carried out similar research on the cooperation between a cell and a battery without the use of DC-DC regulators [19]. In the system with PEM cells, diodes were used instead of the DC-DC converter. The hybrid system consisted of a Horizon H100 fuel cell with a power of 100 W and a Hyperion G3 3300 mAh battery (LiPo – *Lithium-Polymer Battery*) with a voltage of 9.6–12.6 V. The range of the common voltage curve was set at 12.8 to 16.8 V.

Analysis of three variants of drive systems [15] containing successively a basic system, one expanded with an ultracapacitor, and one expanded with an ultracapacitor and a DC-DC converter. The highest drive system efficiency (58.9%) was demonstrated for the variant

containing only the ultracapacitor as extension. In the basic system, the range of power generated by the fuel cell was in the range 0–77 W, while in the system with the highest efficiency this was 14–27 W. Despite the use of semiconductor diodes, it was found that their use in the hybridization of fuel cells with a battery does not utilize the full characteristics of the electric motor and the fuel cell to operate over a wide voltage range.

The performance tests of a one-seat FCHEV vehicle equipped with a 1 kW fuel cell over a distance of up to 31 km in six real-life tests were conducted by Chen et al. [10]. A significant increase in the output voltage while starting and stopping the vehicle, closely related to the current intensity and hydrogen pressure, was observed. Additionally, the large influence of the ambient temperature on the output parameters of the system was noted. The drive system response time is also important. The research results of tests on a Toyota Mirai [23] have shown that the maximum fuel cell voltage of 315 V was achieved after 4 seconds after vehicle start. The maximum power generated by the drive system during acceleration was available 3.5 seconds after vehicle start.

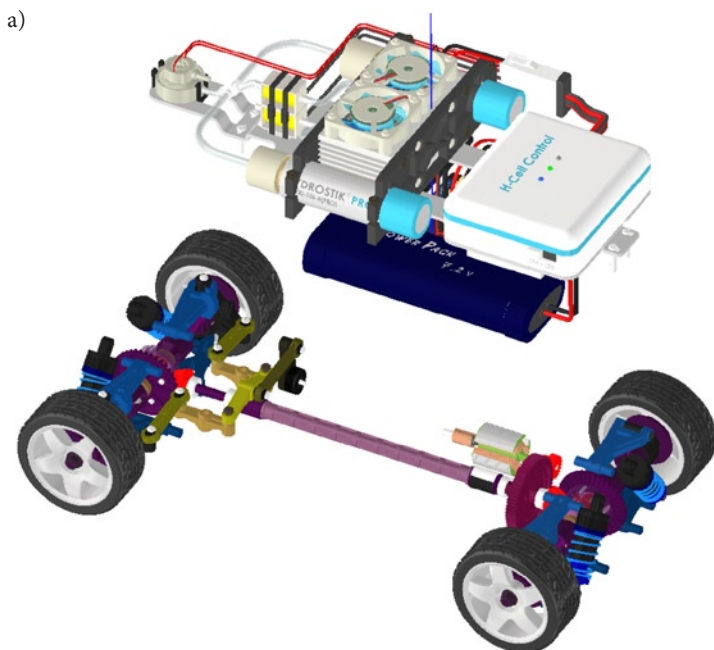
The research described by the authors of this article was also carried out without the use of a DC-DC converter and while using a drive system model.

This article focuses on the energy flow analysis in a drive system model based on test measurement results. The basic identification of a hybrid powertrain equipped with a fuel cell and a battery will form the basis for further research on energy management system optimization. It is not common to conduct experimental studies of this type, and the identification of phenomena occurring in the drive system can be extremely valuable due to its potential towards validating simulation tests.

2. Research aim

Most of the research discussed above concerns simulation studies or stationary studies. In this publication, the authors extend the cooperation of batteries and fuel cells to micro-scale road tests. Although these are not full-scale tests, they allow for a preliminary assessment of energy flow as well as a demonstration of the right conditions for the optimal use of such drive systems.

The aim of the performed research was to evaluate the energy flow in the hybrid drive system in which batteries and fuel cells cooperated at different battery charge states and hydrogen tanks fill levels.



The energy transfer from the fuel cell, which enables the battery to be charged in the hybrid drive system, was also assessed.

3. Research method

3.1. Test vehicle

The energy flow tests were carried out using a model (1:10 scale) of the FCAT-30 hybrid vehicle – equipped with a 30 W fuel cell and a nickel-metal hydride (NiMH) electrochemical battery – operating as a parallel hybrid drive system (Fig. 1). The PEM fuel cell is powered by hydrogen stored in two tanks (in the form of metal hydrides – *Hydrostik*) with a volume of 10 dm³, operating at a pressure of 3 MPa (when fully charged). The vehicle’s electric motor transmits drive to both axles. The technical data of the vehicle and its components are included in Table 1.

The diagram of energy flow in the FCAT-30 hybrid drive system was shown in Fig. 2. The structure of the system enables the parallel supply of the electric motor from two energy sources – the fuel cell and the battery.

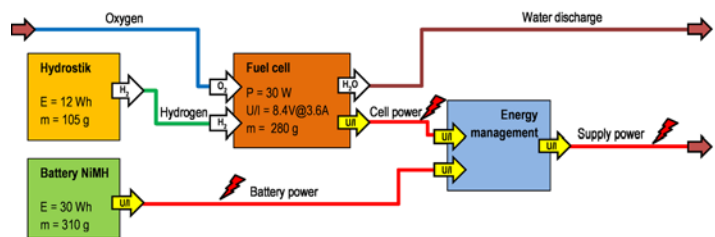


Fig. 2. Diagram of energy flow in a hybrid drive system

The vehicle was powered by the Mabuchi RS-540SH-7520 electric motor supplied with a voltage in the range 4.8–7.2 V. The engine achieves its maximum efficiency of 67% at the following operating parameters: $P = 63.2 \text{ W}$, $n = 19,740 \text{ rpm}$, $I = 13 \text{ A}$, $M_o = 30.6 \text{ mNm}$.

The energy flow (of cells – FC, battery – BATT, system – OUT) in the drive system during the operation of the fuel cell and the battery were calculated using the following equations:

- Instantaneous power:

$$P = U \cdot I \quad (7)$$

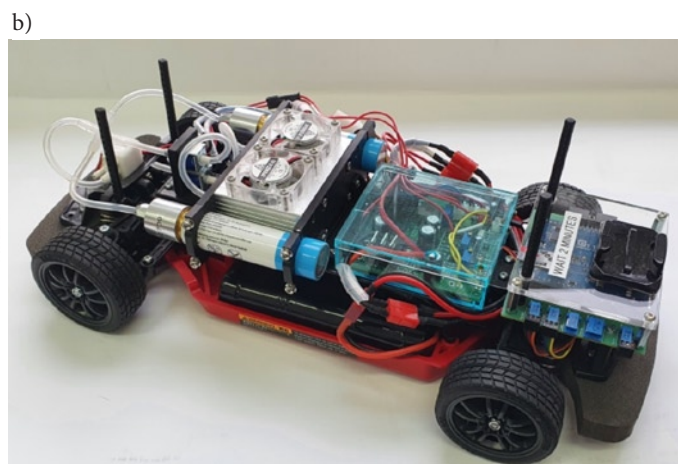


Fig. 1. Vehicle with a hybrid drive powered by a fuel cell and a battery: a) drive diagram with a separately shown fuel cell, b) view of the complete vehicle

Table 1. Vehicle model technical parameters

Parameter	Unit	Value
Fuel cell		
Fuel cell type	-	PEM
Number of cells	-	14
Power	W	30
Hydrogen pressure	MPa	0.045-0.055
Cell stack mass	g	280
H ₂ flow at maximum Ne	dm ³ /min	0.42
System efficiency	%	40 (at max power)
Battery		
Type	-	NiMH
Max output voltage	V	7.2
Electric capacity	mAh	4200
Hydrogen storage		
Tank volume	dm ³	10
Purity	%	≥ 99.995
Form of storage	-	AB5 – metal hydrides
Tank pressure	MPa	3.0
Tank dimensions	mm × mm	φ22 × 88

- Energy Transfer Efficiency:

$$ETE = \frac{P_{OUT}}{P_{FC} + P_{BATT}} \quad (8)$$

- Energy flow:

$$\Delta E = \int_{t=0}^{t=t_{max}} U \cdot Idt \quad (9)$$

The instantaneous values of the energy flow ΔE_i were divided according to the following criteria:

- Discharge of the battery and the fuel cell:

$$\Delta E_{dis} = \int_{t=0}^{t=t_{max}} U \cdot Idt \quad (\text{if } \Delta E_{FC} < \Delta E_{OUT}) \quad (10)$$

- Battery charging:

$$\Delta E_{ch} = \int_{t=0}^{t=t_{max}} U \cdot Idt \quad (\text{if } \Delta E_{FC} > \Delta E_{OUT}) \quad (11)$$

where: U – voltage [V], I – current [A], dt – time [h]

3.2. Test conditions

The research was carried out according to two variants:

- variable speed driving: the distance covered was 530–560 m; the vehicle operated in its full speed and acceleration range;

- acceleration of the vehicle from 0 km/h to the maximum travel speed; the drive lasted four seconds at a maximum acceleration; the distance covered was 28 m.

In the first variant, two laps were performed with the use of different levels of battery charge and hydrogen levels in the tanks, up to and including no hydrogen; in the second – travelling only one way. The vehicle moved on several straight road sections and sections simulating obstacles requiring changes in driving speed (Fig. 3). Such variable conditions reflect those similar to typical road traffic to a much greater extent.

The following parameters were recorded during the drive tests: time, distance traveled, voltage and current intensity of NiMH battery and the fuel cell, as well as voltage and current at the output of the drive system.

4. Results and analysis

4.1. Drive with varying speed

Two test laps were performed in accordance with the designated closed-loop track. Both drives were carried out one after another in a room that ensured no significant air movement and stable climatic conditions that would not impact the driving conditions during the tests. The vehicle speed was recorded in real time during the drive, and it was shown in Figure 4a as a function of the travel time. Both laps took less than 3 minutes to complete, of which route 2 took 11.3 seconds less. The mean speed of the first route was 10.5 km/h and was by 1.4 km/h lower than for the second lap. The maximum speed of both laps was similar and amounted to about 25 km/h. Temporary stops were caused by the loss of stability of the track, especially during route 1. Due to the configuration of the track and the tire grip to the ground, smooth driving was not possible.

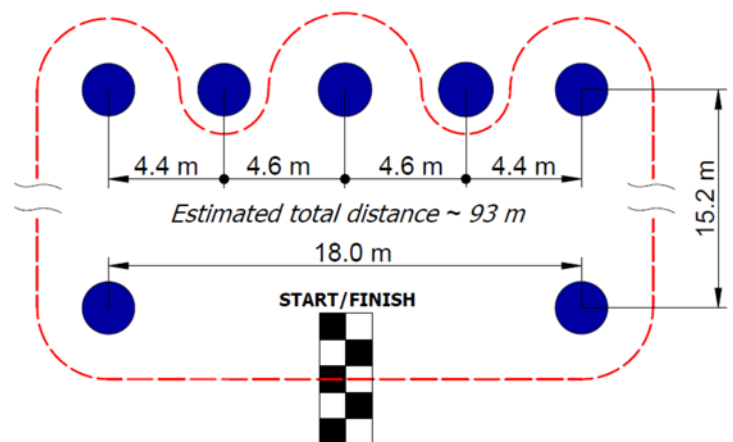


Fig. 3. Vehicle path diagram (estimated length of one lap – approx. 93 m)

Figure 4b is a representation of the battery voltage for the first (green) and second (red) route. Below the voltage curve, the direction of the energy flow was shown on the same diagram represented by two values, the value 1 means charging the battery from the fuel cell, while for the value 0, the fuel cell does not transfer energy to the battery. The operation of the fuel cell allowed maintaining the voltage value during the test laps, mostly above the nominal voltage of the battery of 7.2 V. The mean voltage recorded during the test was 7.9 V and 7.5 V for the first and second laps, respectively. The second route was characterized by much greater voltage fluctuations related to rapid acceleration, thus leading to a more frequent share of battery charging. Differences in the times and rates of charging mode activation were noted between the two routes. The first route was character-

ized by a shorter overall battery charging time and occurring in wider and less consistent intervals, in contrast to the second route where the battery was in charging mode at regular time intervals and the process took more time overall. The share of battery charging time was 22.1% and 25.2% for laps one and two, respectively. Thus indicating higher consumption of energy stored in the battery for the second route. Driving at a stable speed in the initial period of the drive in route 1 shows no charging of the battery by the fuel cell. The reason for this is that the fuel cell covers the energy demand of the drive system to a sufficient extent.

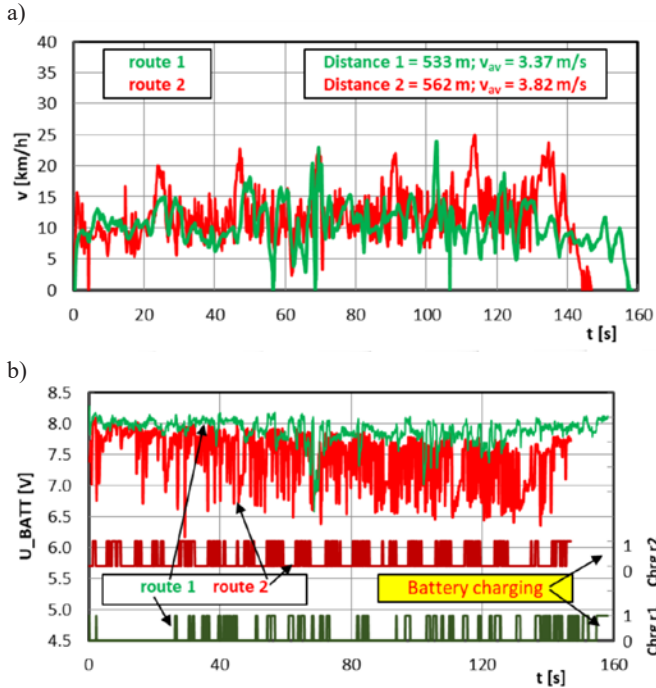


Fig. 4. Test conditions (a) and changes in the battery voltage and its charging profiles (b)

The measuring system (which the vehicle was equipped with) enabled the recording of the voltage and current intensity of the battery, the fuel cell and the electric motor. Based on the obtained data, the power supplied (-) or returned (+) by the P_BATT battery, the power generated by the P_FC (+) fuel cell and the power supplied to the drive transmission system P_OUT (+) – Fig. 5, was also determined. Additionally the drive train energy transfer efficiency (ETE) was established. It should be noted at this point that the analyzed drive system was not equipped with a braking energy recovery system. When analyzing the power supplied to the transmission system, it can be clearly indicated that route 2 was characterized by greater driving dynamics. In both cases, the maximum power transmitted to the wheels of the vehicle was about 150 W. This value is five times higher than the maximum power of the fuel cell as declared by the manufacturer. When the drive system was operating at high load, the vast majority of the power transmitted to the wheels came from the NiMH battery. This solution also provided a significant reduction in the system's response time to rapid acceleration. The power from the fuel cell is either directly transferred to the vehicle's wheels or split to also charge the battery. By analyzing the two routes in terms of the power generated by the fuel cell, dynamic driving (route 2) determines the two-state operation of the fuel cell (between no power generated and the maximum power output – 30 W). In route 1, the cell's power curve appears more stable, and the cell deactivation was limited to a few single events. The mean power generated by the fuel cell for the first and second route were 17 and 12 W respectively. Thus, reducing the amount of sudden changes in vehicle speed increases the share of the cell's power that is transmitted directly to the drive system. Conversely, increasing the driving dynamics and accelerations also

increases the share of power being drawn directly from the battery, while the power generated by the fuel cell ends up largely transferred to the battery.

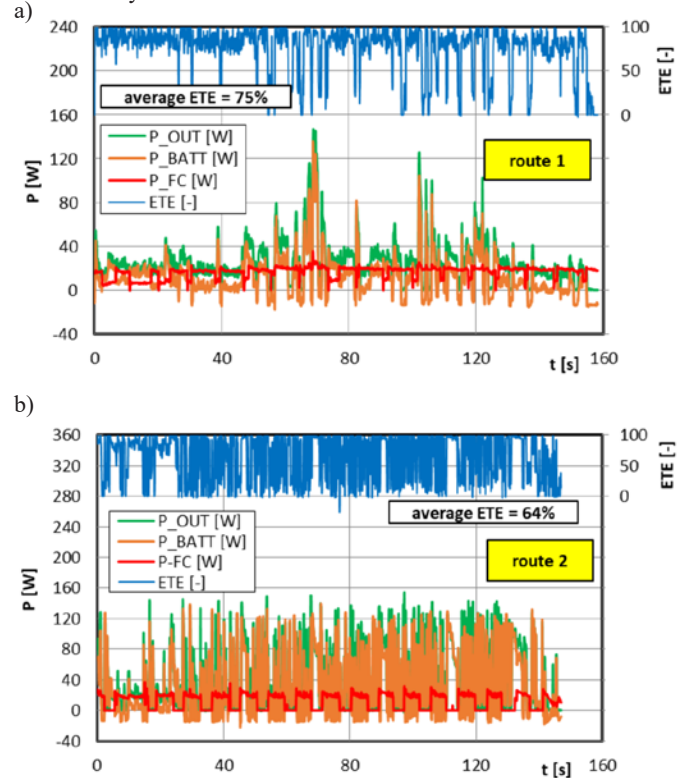


Fig. 5. Conditions for energy flow during the test drives: a) the first route with lower driving dynamics, b) the second route with higher driving dynamics

The energy flow characteristics were determined based on the power generated by the selected components of the drive system with respect to time (Fig. 6). During the first route, a much higher frequency of energy flow changes was observed, while route 2 was characterized only by higher amplitudes. This shows a close relationship between driving dynamics and the intensity of energy transfer between the individual drive system components. The highest amplitudes in the entire time range were obtained for the energy generated by the battery and the energy supplied directly to the drivetrain. The negative energy flow for the battery (meaning its charging) has a greater proportion for route 2 as opposed to route 1 where it is negligible. This confirms the conclusions of the previously discussed results. Energy flow data is particularly important in terms of the selection of the appropriate electrical devices connecting the analyzed elements of the drive system.

The energy balance of the system was obtained as shown in Figure 7 by summing together the amount of energy transferred between the monitored drive system elements. The total amount of energy used during tests in route 1 with lower dynamics was 1612 J lower than during route 2. Moreover, for route 1, a much larger part of the energy was transferred from the fuel cell directly to the vehicle wheels. Increasing driving dynamics resulted in a reduction in the amount of energy transferred from the fuel cell as well as increasing the share of energy transferred towards battery charging (up to 45%). In both cases, only a small part of the energy is used to recharge the battery (12% and 8% for laps 1 and 2 respectively). The algorithm controlling the energy flow between the elements of the drive system did not change throughout the drive tests, hence the large differences in the amount of energy obtained from hydrogen conversion. A greater than double difference indicates the necessity to intervene in, and modify the control system in order to increase the share of energy obtained from the fuel cell during operation even with high load. The lack of additional sensors, e.g. temperature on individual elements of the sys-

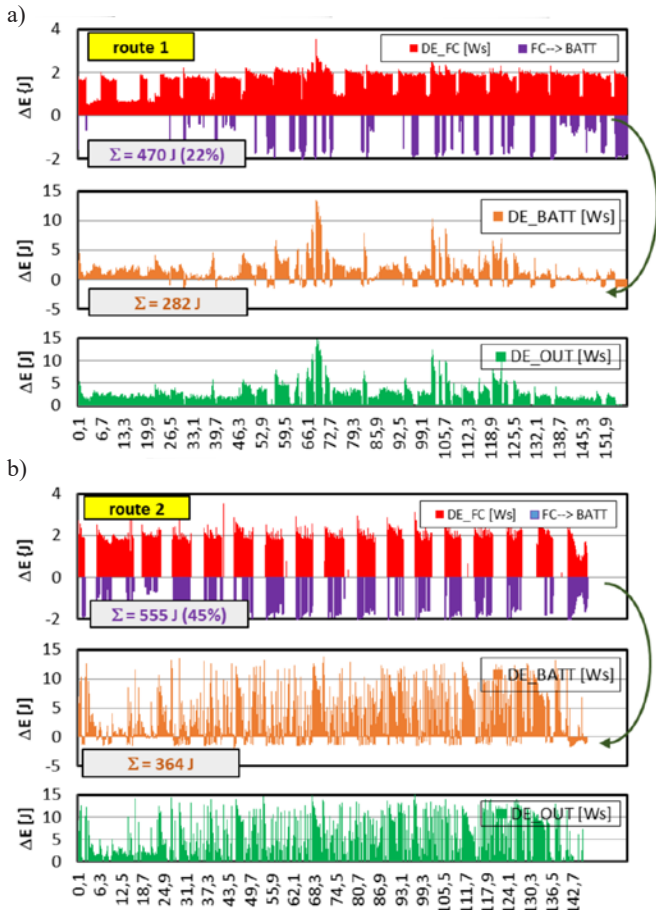


Fig. 6. Instantaneous energy flows in the drive system for a parallel connection of the battery with the fuel cell: route 1 – fully charged battery and full hydrogen container; b) discharged battery

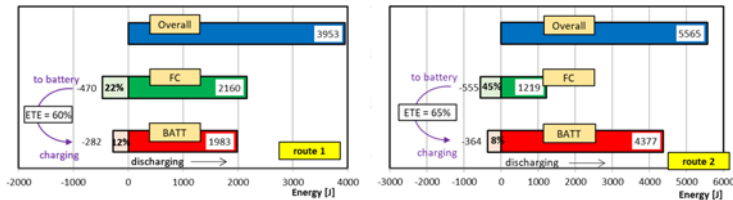


Fig. 7. Assessment of energy flow in a hybrid drive system with a fuel cell and a battery

tem or a hydrogen pressure sensor, does not allow to determine the size of the necessary changes in the control system.

4.2. Vehicle acceleration

As part of the research on the interaction between the fuel cell and the electrochemical battery, the vehicle energy flow during acceleration was also analyzed. The test consisted of accelerating from standstill ($v_0 = 0$ m/s) to the maximum vehicle speed. The tests concerned a case study for a situation in which the hydrogen in the tank would run out and its supply to the fuel cell was cut off. The test conditions concerned the first four seconds of the drive system operation – Fig. 8. During this test, the maximum speed of 7.8 m/s was obtained, which corresponds to 28.1 km/h. The maximum acceleration of the vehicle was recorded during its start, which then decelerated.

During acceleration, the intended effect of such tests was achieved – no hydrogen supply to the fuel cell – Fig. 9. The analysis of the test results (Fig. 9) shows that in the initial phase of acceleration, only 8% of the energy was supplied from the fuel cell. However, as the vehicle speed increased, the share of battery energy supplied also decreased – which can be seen in the range $t = 0.6$ – 1.6 s. During this time, the

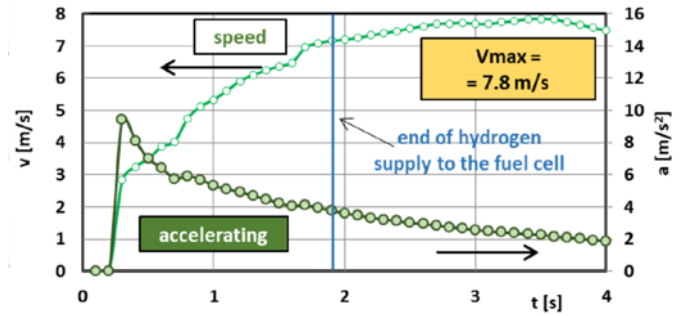


Fig. 8. Changes in test vehicle speed and acceleration during the hybrid drive test

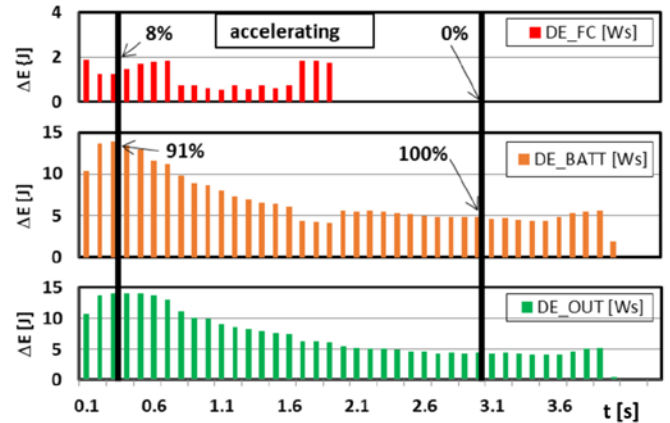


Fig. 9. The energy supply change between the fuel cell (FC), battery (BATT) and the change of energy at the output of the drive system (OUT)

share of fuel cell energy supply increased ($t \sim 0.3$ – 0.6 s), and then it decreased sharply. During $t = 1.1$ s from the start, 93.5% of the energy transferred to the wheels of the vehicle came from the battery, and 6.5% from the fuel cell. Despite the reduction of the total energy of the system from 14 J ($t = 0.3$ s) to 9 J ($t = 1.1$ s) during acceleration, the energy shares of both systems remained almost unchanged. It is interesting that once the hydrogen supply ran out, its energy share in powering the vehicle in the last moments of the fuel cell operation was about 30% (1.77 J – fuel cell in relation to 4.14 J – battery).

Cutting off the hydrogen supply during acceleration results in an increase in energy consumption from the battery by about 35% (from time $t = 2$ s) – Fig. 10. Such values are sufficient to obtain a further increase in speed from 7.2 m/s (at $t = 2$ s) to 7.8 m/s (at $t = 3.4$ s).

The interaction between the fuel cell system and batteries described above indicates the possibility of continuing the drive's operation (including its further acceleration) even when the hydrogen supply to the fuel cell is cut off.

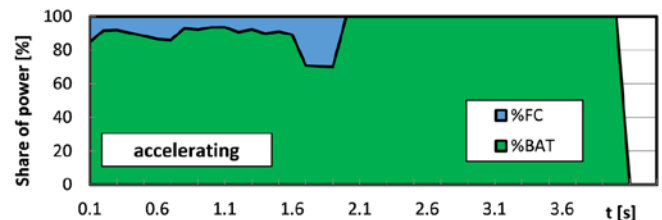


Fig. 10. Share of power supplied by the battery and the fuel cell while accelerating and when the fuel cell hydrogen supply is cut off

The analysis of the battery and fuel cell energy supply share indicate much higher values of the battery share, which is related to the end of the fuel cell operation. Under these conditions of vehicle

acceleration, the share of the fuel cell in power supply to the drive system was only 8%. Based on the data in Fig. 11, it can be shown that the efficiency of energy transmission from both driving sources (battery and fuel cell) was about 95%. Typical driving conditions showed much lower values of this efficiency, measured in the range of 64–75% (data included in Fig. 5). This means that the maximum use of the energy of both vehicle power supply devices was carried out with much greater energy efficiency.

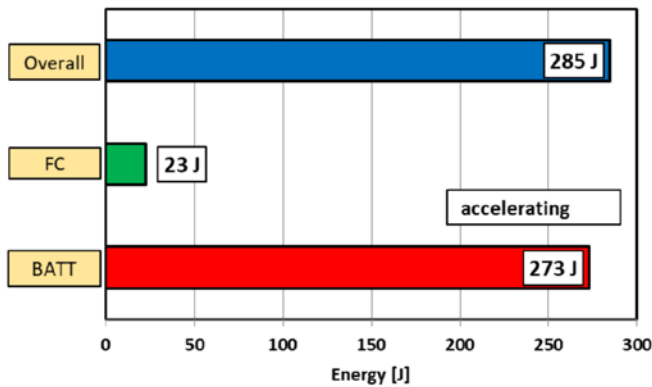


Fig. 11. The total energy contributions of the fuel cell and the battery during the acceleration of a vehicle powered by a hybrid system

5. Conclusions

This article presents the results of experimental tests of a model vehicle drive system (1:10 scale) consisting of a PEM fuel cell and a NiMH battery. The tests included recording six operating parameters

of the drive system during two test runs over a total distance of about 600 m and one acceleration test. Based on the observations made, the following conclusions were presented.

1. The driving dynamics has a significant impact on the energy flow between the drive system components (fuel cell, battery, electric motor).
2. Increasing driving dynamics results in an energy consumption increase by 29%, a reduction in energy transfer from a fuel cell by 43.6% and an increase in the share of energy intended for battery charging by 23%.
3. Lower driving dynamics (route 1) increased the energy transmission efficiency to the drive system by 11% and reduced the energy transmission efficiency from the fuel cell to the battery by 5%.
4. In situations of large, rapidly changing drive system load values, the battery was the main source of energy.
5. Increasing the share of energy obtained from hydrogen processing under high load conditions requires modification of the vehicle control system and extending the scope of tests by measuring additional selected parameters (temperature, pressure).
6. Continuous operation of the drive system in full power mode allowed to achieve a much higher efficiency of energy transmission to the drive system (95%) compared to the system operation in variable conditions of 64–75%.

References

1. Affam A, Buswig Y M, Bin Hj Othman A K, Julai N B, Qays O. A review of multiple input DC-DC converter topologies linked with hybrid electric vehicles and renewable energy systems. *Renewable and Sustainable Energy Reviews* 2021; 135: 110186, <https://doi.org/10.1016/j.rser.2020.110186>.
2. Akinyele D, Olabode E, Amole A. Review of fuel cell technologies and applications for sustainable microgrid systems. *Inventions* 2020; 5 (3): 42, <https://doi.org/10.3390/inventions5030042>.
3. Ali M S, Kamarudin S K, Masdar M S, Mohamed A. An overview of power electronics applications in fuel cell systems: DC and AC converters. *The Scientific World Journal* 2014; 103709, <https://doi.org/10.1155/2014/103709>.
4. Balci Ö, Karagöz Y, Kale S, Damar S, Attar A, Köten H, Dalkılıç A S, Wongwises S. Fuel consumption and emission comparison of conventional and hydrogen feed vehicles. *International Journal of Hydrogen Energy* 2020; <https://doi.org/10.1016/j.ijhydene.2020.11.095>.
5. Bauman J, Kazerani M. A comparative study of fuel-cell-battery, fuel-cell-ultracapacitor, and fuel-cell-battery-ultracapacitor vehicles. *IEEE Transactions on Vehicular Technology* 2008; 57 (2): 760-769, <https://doi.org/10.1109/TVT.2007.906379>.
6. Bhatt M D, Lee J Y. High capacity conversion anodes in Li-ion batteries: A review. *International Journal of Hydrogen Energy* 2019; 44 (21): 10852-10905, <https://doi.org/10.1016/j.ijhydene.2019.02.015>.
7. Borucka A, Wiśniowski P, Mazurkiewicz D, Świdorski A. Laboratory measurements of vehicle exhaust emissions in conditions reproducing real traffic. *Measurement* 2021; 174: 108998, <https://doi.org/10.1016/j.measurement.2021.108998>.
8. Brzeżański M, Rodak Ł. Investigation of a new concept of hydrogen supply for a spark-ignition engine. *Combustion Engines* 2019; 178 (3): 140-143, <https://doi.org/10.19206/CE-2019-324>.
9. Changizian S, Ahmadi P, Raeesi M, Janavi N. Performance optimization of hybrid hydrogen fuel cell-electric vehicles in real driving cycles. *International Journal of Hydrogen Energy* 2020; 45 (60): 35180-35197, <https://doi.org/10.1016/j.ijhydene.2020.01.015>.
10. Chen K, Laghrouche S, Djerdir A. Performance analysis of PEM fuel cell in mobile application under real traffic and environmental conditions. *Energy Conversion and Management* 2021; 227: 113602, <https://doi.org/10.1016/j.enconman.2020.113602>.
11. Dimitriou P, Tsujimura T. A review of hydrogen as a compression ignition engine fuel. *International Journal of Hydrogen Energy* 2017; 42 (38): 24470-24486, <https://doi.org/10.1016/j.ijhydene.2017.07.232>.
12. Farhani S, Barhoumi E M, Bacha F. Design and hardware investigation of a new configuration of an isolated DC-DC converter for fuel cell vehicle. *Ain Shams Engineering Journal* 2020; 12 (1): 591-598, <https://doi.org/10.1016/j.asej.2020.07.014>.
13. Fayaz H, Saidur R, Razali N. An overview of hydrogen as a vehicle fuel. *Renewable and Sustainable Energy Reviews* 2012; 16 (8): 5511-5528, <https://doi.org/10.1016/j.rser.2012.06.012>.
14. Feroldi D, Serra M, Riera J. Design and analysis of fuel-cell hybrid systems oriented to automotive applications. *IEEE Transactions on Vehicular Technology* 2009; 58 (9): 4720-4729, <https://doi.org/10.1109/TVT.2009.2027241>.
15. Grady P, Chen G, Verma S, Marellapudi A, Hotz N. A study of energy losses in the world's most fuel efficient vehicle. 2019 IEEE Vehicle Power and Propulsion Conference (VPPC), Hanoi, Vietnam, IEEE: 2019: 1-6, <https://doi.org/10.1109/vppc46532.2019.8952212>.
16. Guo F, Qin J, Ji Z, Liu H, Cheng K, Zhang S. Performance analysis of a turbofan engine integrated with solid oxide fuel cells based on Al-H₂O hydrogen production for more electric long-endurance UAVs. *Energy Conversion and Management* 2021; 235: 113999, <https://doi.org/10.1016/j.enconman.2021.113999>.

- org/10.1016/j.enconman.2021.113999.
17. Gurz M, Baltacioglu E, Hames Y, Kaya K. The meeting of hydrogen and automotive: a review. *International Journal of Hydrogen Energy* 2017; 42 (36): 23334-23346, <https://doi.org/10.1016/j.ijhydene.2017.02.124>.
 18. Haseli Y. Maximum conversion efficiency of hydrogen fuel cells. *International Journal of Hydrogen Energy* 2018; 43 (18): 9015-9021, <https://doi.org/10.1016/j.ijhydene.2018.03.076>.
 19. Howroyd S, Chen R. Powerpath controller for fuel cell & battery hybridisation. *International Journal of Hydrogen Energy* 2016; 41 (7): 4229-4238, <https://doi.org/10.1016/j.ijhydene.2016.01.038>.
 20. Innocenzi V, Ippolito NM, De Michelis I, Prisciandaro M, Medici F, Vegliò F. A review of the processes and lab-scale techniques for the treatment of spent rechargeable NiMH batteries. *Journal of Power Sources* 2017; 362: 202-218, <https://doi.org/10.1016/j.jpowsour.2017.07.034>.
 21. Khayyer P, Famouri P. Application of two fuel cells in hybrid electric vehicles. *SAE Paper 2008: 2008-01-2418*, <https://doi.org/10.4271/2008-01-2418>.
 22. Manoharan Y, Hosseini S E, Butler B, Alzahrani H, Senior B T F, Ashuri T, Krohn J. Hydrogen fuel cell vehicles; current status and future prospect. *Applied Sciences* 2019; 9 (11): 2296, <https://doi.org/10.3390/app9112296>.
 23. Pielecha I, Cieślak W, Szałek A. The use of electric drive in urban driving conditions using a hydrogen powered vehicle - Toyota Mirai. *Combustion Engines* 2018; 172(1): 51-58, <https://doi.org/10.19206/CE-2018-106>.
 24. Pielecha I, Pielecha J. Simulation analysis of electric vehicles energy consumption in driving tests. *Eksploatacja i Niezawodność - Maintenance and Reliability* 2020; 22 (1): 130-137, <https://doi.org/10.17531/ein.2020.1.15>.
 25. Rana K, Natarajan S, Jilakara S. Potential of hydrogen fuelled IC engine to achieve the future performance and emission norms. *SAE Paper 2015: 2015-26-0050*, <https://doi.org/10.4271/2015-26-0050>.
 26. Shang J, Kendall K, Pollet B G. Hybrid hydrogen PEM fuel cell and batteries without DC-DC converter. *International Journal of Low-Carbon Technologies* 2016; 11 (2): 205-210, <https://doi.org/10.1093/ijlct/ctt070>.
 27. Sorlei I S, Bizon N, Thounthong P, Varlam M, Carcadea E, Culcer M, Iliescu M, Raceanu M. Fuel cell electric vehicles - a brief review of current topologies and energy management strategies. *Energies* 2021; 14: 252, <https://doi.org/10.3390/en14010252>.
 28. Szumska E, Jurecki R, Pawełczyk M. Evaluation of the use of hybrid electric powertrain system in urban traffic conditions. *Eksploatacja i Niezawodność - Maintenance and Reliability* 2020; 22 (1): 154-160, <https://doi.org/10.17531/ein.2020.1.18>.
 29. Verhelst S, Sierens R, Verstraeten S. A critical review of experimental research on hydrogen fueled SI engines. *SAE Paper 2006: 2006-01-0430*, <https://doi.org/10.4271/2006-01-0430>.
 30. Yao G, Du C, Ge Q, Jiang H, Wang Y, Ait-Ahmed M, Moreau L. Traffic-condition-prediction-based HMA-FIS energy-management strategy for fuel-cell electric vehicles. *Energies* 2019; 12: 4426, <https://doi.org/10.3390/en12234426>.
 31. Zhang J, Zhang H, Wu J, Zhang J. *PEM Fuel Cell Fundamentals. PEM Fuel Cell Testing and Diagnosis*, Elsevier: 2013: 1-42, <https://doi.org/10.1016/B978-0-444-53688-4.00001-2>.
 32. Zhao Z, Wang T, Li M, Wang H, Wang Y. Optimization of fuzzy control energy management strategy for fuel cell vehicle power system using a multi-island genetic algorithm. *Energy Science & Engineering* 2021; 9: 548-564, <https://doi.org/10.1002/ese3.835>.